Performance of Vehicle Fuel System Elastomers and Plastics with Test Fuels Representing Gasoline Blended with 10% Ethanol (E10) and 16% Isobutanol (iBu16)

KEYWORDS: Plastic, Elastomer, Compatibility, Ethanol, Isobutanol, Volume, Hardness

ABSTRACT

The compatibilities of fuel system elastomers and plastics were evaluated for test fuels containing 16 vol.% isobutanol (iBu16) and 10 vol.% ethanol (E10). Elastomers included two fluorocarbons, four acrylonitrile butadiene rubbers (NBRs), and one type of fluorosilicone, neoprene, and epichlorohydrin/ethylene oxide. Plastic materials included four nylon grades, three polyamides, polytetrafluoroethylene (PTFE), polyvinylidene fluoride (PVDF), ethylene tetrafluoroethylene (ETFE), polyphenylene sulfide (PPS), high density polyethylene (HDPE), polybutylene terephthalate (PBT), polyloxymethylene (POM), flexible polyvinylchloride (PVC), polyetherimide (PEI), polyetheretherketone (PEEK), and a phenol formaldehyde reinforced with glass fiber. For each polymer material the volume, mass, and hardness were measured before and after drying. Dynamical mechanical analysis (DMA) measurements were also performed on the dried specimens.

For the elastomer materials the measured properties were similar for both fuels. The fluorocarbons and fluorosilicone swelled the least (~20%), while more moderate (20-45%) expansion occurred for the two NBR hose grades and ECO. HNBR, neoprene, and silicone exhibited high swelling and softening which likely precludes their use in many fuel systems. For the plastic materials, the observed swell was low; Nylon 11 swelled around 15%, but otherwise their measured swell was <10%. Many of the plastics also showed sensitivity to alcohol type, as the E10 test fuel often imparted appreciably higher swell than iBu16. In general, the plastic materials showed good compatibility with the iBu16 and E10 test fuels. The sole exception was the PVC material, which was structurally degraded from exposure to either fuel type. Compositional analysis showed high fuel retention in Nylon 12 and PVC. PVC also experienced a significant reduction in plasticizer compounds following exposure, which resulted in embrittlement and an increase in the glass-to-rubber transition temperature.

NOTICE

INTRODUCTION

Biomass-derived fuels are becoming increasingly important as components of transportation fuels in the United States, and in other countries. One key motivation for increasing biofuel use is to reduce petroleum consumption, thereby improving energy security and independence [1]. In addition, biomass, especially corn and sugar cane, is an abundant, renewable, and carbon neutral source of fuel grade alcohols. In the United States, ethanol has been included as a gasoline component at volume concentrations of 10% (E10) since 2011. E10 is approved under the "GasPlus" waiver and also the OCTAMIX waiver guidelines, which allows oxygenates, such as alcohols, to be added to gasoline up to levels which correspond to a 3.7wt.% of oxygen [2]. Any new fuel chemistry or additive must also be compatible with existing fuel system materials before being accepted by the U. S. Environmental Protection Agency (EPA). Current gasoline fueling infrastructure is compatible with E10, and it is expected that new fuel chemistries demonstrate equivalent compatibility performances. Infrastructure materials include many metals, plastics and elastomers. Historically, metals were the predominant material used in fueling systems due to their high mechanical strengths, excellent wear resistances, and durability. More recently, plastics have replaced metals in many applications due to their lower cost and weight. Notable examples include polyvinylidene fluoride (PVDF or Kynar), which makes up the bulk of underground fuel piping, and HDPE, which has replaced steel and aluminum in the construction of most vehicle fuel tanks.

Hydrocarbon fuels, including alcohols, do not directly corrode metals; corrosion is almost always associated with water and other contaminants. However, they can degrade polymers if they are mutually soluble. Failure of a polymeric seal or structural component may lead to fuel leakage, which can create an environmental hazard. The compatibility of polymeric materials with

gasoline-alcohol mixtures has been the subject of several studies [3-13]. These efforts were primarily concerned with the impact of ethanol blends with common elastomers (i.e. fluorocarbon and acrylonitrile butadiene rubbers). However, a study by Durbin et al [13] also included butanol as a test fuel, and plastic materials common to fuel handling systems in gas stations. In each of these investigations the addition of ethanol produced significant volume expansion in the elastomers and more modest swell in the plastics. The addition of 55% butanol (to a gasoline test fuel) resulted in property changes roughly equivalent to or less than those obtained from E10 [13].

Butamax Advanced Biofuels, LLC has developed proprietary technologies to convert corn into isobutanol using the infrastructure already in-place at ethanol production facilities [14]. Isobutanol is of interest since it has a higher energy density relative to ethanol. It is also less volatile and water soluble. Since the oxygen content of isobutanol is lower than ethanol, the amount of isobutanol that can be added to meet the 3.7wt.% requirement is higher than that of ethanol. This translates to 16% isobutanol vs 10% for ethanol. As a result, more biomass can be utilized as a gasoline component, and therefore the impact on petroleum reduction is conceivably higher than it is for ethanol. Compatibility studies of materials with gasoline blends containing isobutanol are limited. In a previous set of experiments, the authors evaluated isobutanol compatibility with metals, elastomers, and plastics used to store and transport fuel in gas stations [15-16]. Many of these same polymers are also present in onboard vehicle fueling (examples include HDPE, nylons, fluorocarbons, and nitrile rubbers), but there are some, such as ECO, PEEK and PEI) that are unique to vehicle fuel systems.

The objective of this study was to examine the compatibility of known polymers used in vehicle fueling systems with test fuels representing E10 and iBu16. Polymers that are in close proximity to the vehicle fueling system, but are not in direct contact with the fuel, were also included since they may inadvertently become exposed through accidental spillage. In order to determine the impact of new fuels, it is necessary to understand the compatibility performance of fuel system elastomers and plastics to new fuel chemistries. The data obtained from these studies can be used to guide material selection and identify potential leak sites in fueling hardware. This paper describes a research project at Oak Ridge National Laboratory (ORNL), supported by Butamax Advanced Biofuels, to evaluate the impact of aggressive fuel formulations representing E10 and 16% isobutanol (iBu16) on polymer materials common to vehicle fueling systems. Data obtained from the prior ethanol compatibility studies on these materials are included for additional interpretation and summary.

MATERIALS

Test Fuels. In this study test fuels representing gasoline blended with 10% ethanol and 16% isobutanol were derived from the aggressive standard formulations in SAE J1681 [17]. The blend containing 10% aggressive ethanol and 16% aggressive isobutanol are denoted as CE10a and CiBu16a, respectively [17]. The letter C in the fuel name refers to the gasoline surrogate, Fuel C, which is a 50:50 blend of isooctane and toluene and is representative of high aromatic grades of gasoline. The aggressive ethanol formulation followed the one outlined in SAE J1681 and was used as the basis for constructing an analogous aggressive isobutanol, which is not included in the standard. Aggressive ethanol contains 99% ethanol, 1% water, 5 ppm sodium chloride, 25 ppm sulfuric acid, and 75 ppm acetic acid. The components making up a

corresponding aggressive isobutanol solution were kept similar to aggressive ethanol, except that isobutanol replaced ethanol and isobutyric acid was substituted for acetic acid.

The formulations for the aggressive methanol and ethanol formulations in SAE J1681 indicate that the molar concentration of the organic acid was kept constant at 0.001 M for both alcohol types. Therefore, in order maintain consistency with the protocol in SAE J1681, a molar ratio of 0.001 M was used to determine the concentration of isobutyric acid in an aggressive isobutanol formulation. By keeping the molar concentration constant, the number of acid protons in a given volume of test fuel is the same for each aggressive alcohol.

The resulting composition used to make 1 liter of the aggressive isobutanol is shown in Table 1. The concentrations of water, sodium chloride, and sulfuric acid matched that of aggressive ethanol, since the processes and handling of isobutanol and ethanol are expected to be similar. The aggressive formulation is conservative by design but is considered to be representative of worst case field conditions since sulfuric and organic acids are present in certain fuels, including ethanol (and are also expected to occur in isobutanol as well). These acids are formed in the production process of ethanol or created via oxidation during handling, transfer, or storage. Sulfuric acid is believed to originate from impurities associated with alcohol fermentation, but it may also be formed by the reaction of fuel-borne sulfur with alcohol and can be particularly corrosive to metals and polymers. Commercial-grade gasoline may contain varying amounts of sulfur (usually <10 ppmw with a maximum of 30 ppmw) , which is usually present as disulfides. Disulfides are converted to sulfonic acids in the presence of atmospheric oxygen and water.

Since water is generally present either as a liquid or as vapor, sulfuric acid will form in ethanol-blended gasoline and possibly in isobutanol blends as well.

These test fuels are designed to simulate severe, real-world conditions. They are also intended to minimize the exposure time necessary to rigorously evaluate materials while providing a standard method of testing fuel system materials. Fuel C was selected as the control since it represents premium gasoline and is a widely used standard test fluid for studying material compatibility to gasoline.

The test fuels were prepared by splash-blending the components one at a time. The first step was to prepare the aggressive water solution, which was poured into an empty 30-gal drum. Completed denatured ethanol (CDA 20) or reagent-grade isobutanol was added to the aggressive water solution followed by the appropriate volume of Fuel C. The final fuel formulation was poured into the exposure chamber, which had been preloaded with the material specimens. Visual observation indicated that the resulting fuel mixture was single phase.

Elastomer Materials. The elastomer materials evaluated in this study included two fluorocarbons (Viton A401C and Viton B601), and one type of fluorosilicone, neoprene, hydrogenated acrylonitrile butadiene rubber (HNBR), a blend of NBR and PVC (OZO), epichlorohydrin/ethylene oxide (ECO), and silicone. A list of these elastomers and their applications is shown in Table 2. As seen in the table, many of these elastomer materials are common o-ring materials. NBR (SE grade) is a common hose material in small engine applications, while NBR (GD grade) is a legacy hose material for many gasoline dispensers. The other two NBR materials (HNBR, and OZO) and neoprene are also legacy elastomer materials that may exist on some older vehicles, while fluorocarbon and fluorosilicone are considered

advanced, high-performance elastomers with improved compatibility to alcohols. Although silicone is not common in vehicle fueling systems, it is frequently used in small engine fuel systems, which are often fueled with E10. For each elastomer type, three specimens were evaluated. The length, width, and thickness for each were 3.8, 1.3, and 0.2 cm (1.5, 0.5, and 0.08 in.), respectively.

Plastic Materials. Eighteen plastic materials were evaluated in this study. As listed in Table 3, they included four nylons, three polyamides, three fluoroplastics (polytetrafluoroethylene, polyvinylidene fluoride, and ethylene tetrafluoroethylene), polyphenylene sulfide (PPS), high density polyethylene (HDPE), polybutylene terephthalate (PBT), polyoxymethylene (POM), polyvinyl chloride (PVC), polyetherimide (PEI), polyetheretherketone (PEEK) and a phenol formaldehyde reinforced with glass fiber (GFPF). As stated previously, many of these plastics have replaced steel and aluminum traditionally used in housings, tanks and pump components. Conventional fuel tanks are primarily composed of high-density polyethylene (HDPE) with one or more of the polyamides as a permeation barrier liner. Other materials, such as PBT, PVC, PEEK and GFPF are not necessarily used in direct contact with the fuel, and therefore do not contribute to the risk of fuel leakage, but they do provide protection to other critical engine components that can be adversely affected by direct contact with fuel due to spillage, etc. As a result, these protective coating materials are important to ensure the warranty and durability performance of the engine and other under the hood components. For each plastic type, three specimens were prepared from commercial stock sheets. Each specimen measured 2.54 cm (1 in.) wide, 7.6 cm (3 in.) long, and 0.32 cm (0.125 in.) thick. These specimens were submerged in the test fuel liquid for 16 weeks.

EXPERIMENTAL

The exposure conditions were determined from earlier studies which showed that full saturation of elastomeric and plastic material specimens was achieved for exposure durations of 4 and 16 weeks, respectively [18]. A test temperature of 60^{o}C was selected to be consistent with the dispenser test protocol used by Underwriters Laboratories [19]. A flow chart highlighting the exposure and measurement protocols is shown in Figure 1. The volume change for the elastomer specimens was determined using the protocol described in ASTM D471-06 [20], while the those for the plastics were determined by direct measurement of the specimen geometry. The hardness measurements were performed according to ASTM D2240 [21]. The Shore A method was used for the elastomers and the Shore D method was used for the plastics. The actual specimen thicknesses were less than the 0.635 cm specification in ASTM D2240 for Shore D measurements, but since hardness measurements for unexposed specimens matched the values provided by the suppliers, the tested specimens thicknesses were deemed acceptable. A total of five hardness measurements were made on each specimen. The measurement locations were the four corners and the center.

The specimens were loaded and sealed inside a specially-designed chamber (the details of which have been covered in a previous report) [18]. Three specimens of each material were completely submerged in the test fuel liquids for 4 weeks. Prior to test fuel exposure, specimens were measured for mass, volume and hardness. Following the exposure runs, the specimens were removed and maintained in the wetted state prior to measurement. The wetted specimens were remeasured for mass, volume and hardness and then dried at 60^{o}C in an open furnace. The drying times for the elastomers and plastics were 20 hours and 65 hours, respectively. After drying, the

samples were remeasured for mass, volume and hardness. The changes in these properties from the original (untreated) condition were used to assess compatibility.

The dried specimens were evaluated via dynamic mechanical analysis (DMA) testing to further evaluate whether any structural changes had taken place in the polymers following exposure to the test fuels. DMA measures the storage modulus as a function of temperature and is used to determine the onset of the glass to rubber transition of polymers. A simplified representative DMA graph is shown in Figure 2. At low temperatures, all polymers will be in a rigid glassy state due to molecular binding. As the temperature is increased, a transition point occurs associated with a sharp drop in modulus. At this point the polymer molecular chains become more flexible and the material transitions to a more pliable rubbery state. The temperature associated with this onset is known as the glass transition temperature, T_g. The ability to flex and deform is important in sealing applications and the lower operational limit of elastomers is dictated by T_g. Similarly, rigid plastic materials used in structural applications are designed to operate in the glassy region. Therefore, T_g defines the upper operational limit of most structural plastics. T_g is an important property since it is sensitive to any microstructural change that has occurred to the polymer structure. Any shift in T_g that shrinks the operational range of an elastomer or plastic material may result in failure if the temperature falls outside the expected design range.

RESULTS

At the end of the exposure periods, all of the polymer specimens were found to be structurally intact after removal from either test fuel. For each material type and test fuel, the measured volumes and hardness values were observed to be highly consistent as indicated by the narrow

ranges of error (which are included in the figures). To better elucidate the relationship between mass and volume for each material, the volume change results are also compared with the corresponding mass change values.

Elastomers

The wetted volume results are shown in Figure 3 for each elastomer material and test fuel. In general, the elastomers' responses with either test fuel were similar, but the NBR/PVC blend, silicone and ECO underwent slightly lower expansion in CiBu16a than in CE10a. This slight improvement is attributed to the lower polarity of isobutanol relative to ethanol. As seen in Figure 3 the two fluorocarbons and the fluorosilicone showed the best compatibility (i.e. lowest swell) of the elastomer materials. The four NBR grades exhibited different performances depending on the grade. The volume increases for the two NBR hose materials, NBR (SE Grade) and NBR (GD Grade), and the NBR/PVC blend were between 20 and 40% and are considered moderate. In contrast HNBR swelled to over 80% indicating that this elastomer would not likely be acceptable for many hose and seal applications. ECO, neoprene, and silicone swelled to 42%, 89%, and 140%, respectively. The levels of volume expansion exhibited by these materials, especially neoprene and silicone, are considered high. It is important to note that none of these three elastomers are common to modern fueling systems, though they may exist on some legacy systems. The corresponding point change in hardness results for the elastomers in the wetted state show pronounced softening as depicted in Figure 4. This observation is consistent with fluid ingress as the absorbed fluid provides little to no resistance to applied stress, thereby lowering the overall strength and modulus of the polymer. For the wetted elastomers, the observed volume expansion correlated closely with the mass gain as can be seen in a plot of the volume and mass as shown in Figure 5. The resulting data shows a strong linear relationship between the wetted volume and

mass which is independent of the test fuel type. This result indicates that, for the wetted elastomers, the level of swell depends predominantly on the mass of the absorbed fuel.

The dried volume change results for the elastomers are shown in Figure 6 and the accompanying point change in hardness results are shown in Figure 7. The two fluorocarbons (Viton A401C and Viton B601) retained a small portion of the test liquids within their molecular structures which contributed to a slight expansion (over baseline) in the dried state. This expansion was slightly higher for the specimens exposed to isobutanol blend. This effect is attributed to the lower volatility of isobutanol which would require longer drying time or higher temperatures than ethanol. In addition, isobutanol, being a larger molecule than ethanol, would also be less diffusive in the polymer structure. These retained fluids also imparted the low levels of softening shown in Figure 7.

Neoprene, along with NBR (SE Grade), NBR (GD Grade), and the NBR/PVC blend showed a pronounced decrease in volume and mass following drying. This finding confirms the dissolution and subsequent extraction of one or more additive components from these elastomer materials, which are normally heavily compounded with plasticizers to improve pliability. As seen in Figure 7, these four materials all exhibited significant increases in hardness (embrittlement) after drying, indicating plasticizer extraction. In contrast the measured volumes, masses, and hardness results of fluorosilicone, HNBR, silicone, and ECO returned to values approaching baseline. Here, the implication is that these materials are not heavily compounded with additive components. A plot of the volume versus the mass change for the dried elastomers (Figure 8) yielded a linear relationship between volume and mass. However, in contrast to the wetted elastomer materials, there is more scatter in the results; possibly due to variability in drying completeness.

The glass transition temperatures (T_gs) for the elastomer materials are shown in Figure 9. For each material type, the results are shown for the starting baseline condition and for exposure to the two test fuels. For many of the elastomer materials, the T_g values were not significantly affected by exposure to the test fuels, though small increases of 10 to 20 degrees Kelvin in were noted for NBR (SE grade), NBR (GD grade) and the NBR/PVC blend. This increase is attributed to the dissolution and extraction of the plasticizer additive that was apparent from Figures 6 and 7.

Plastics

The wetted volume change results are shown in Figure 10 for the nylons and polyamides and in Figure 11 for other plastic materials. Nylon 6, Nylon 6/6, PARA, and the two PPA grades showed either negligible or slight (<2%) expansion with exposure to CiBu16a. In contrast, Nylon 11 and Nylon 12 exhibited moderate volume expansion with the CiBu16a test fuel. For Nylon 11, Nylon 12, and PPA (Solvay Amodel), the volume changes accompanying CE10a exposure were roughly equivalent to CiBu16a. For the other plastics in this grouping, the CE10a test fuel produced significantly higher volume swell (4-9%) than did CiBu16a (<2%). As seen in Figure 11, PPS, PTFE, PEI, PEEK and GFPF showed negligible-to-slight volume increases with either test fuel. PVDF and ETFE showed a small 3% increase in volume, while moderate (~5 -10%) expansion was noted for PBT, HDPE, and POM. Of these, only PBT showed appreciably higher swelling in CE10a, while the volume change results were roughly equivalent for the other plastics. PVC differed from the other plastics by exhibiting a substantial (>20%) volume reduction from the baseline value. Because the PVC material was partially dissolved by the test fuels, its use with gasoline containing ethanol or isobutanol is not recommended. Comparison of the volume change with the corresponding change in mass can be seen in Figure 12. As with the elastomers, a strong linear relationship exists between the measured volume and mass that is predominantly

independent of elastomer type and fuel chemistry. The one notable exception is Nylon 12, which is represented by the two data points that deviate from this general linearity.

The corresponding wet hardness results are shown in Figures 13 and 14. For most plastic materials the measured reduction in hardness (or increased softening) corresponded with the level of absorbed fuel as expected. Both fuel types performed similarly, though slightly less softening was noted for specimens exposed to CiBu16a. A significant reduction in hardness occurred in the PVC material, which when considered along with the measured shrinkage indicates that this material was structurally degraded by both test fuels.

The volume change results for the plastics after drying at 60^{o}C for 65 hours are shown in Figures 15 and 16. In general the volumes for the nylons and polyamides returned to their baseline values for those specimens exposed to CiBu16a, while appreciable (>4%) swelling remained for the CE10a exposures. Notable exceptions were Nylon 11, which exhibited a higher volume (fuel retention) with CiBu16a, and Nylon 12, which lost volume and mass in both fuels. The Nylon 12 shrinkage is attributed to dissolution and extraction of one or more key additives. The corresponding hardness measurements (Figures 17 and 18) also approached the starting baseline values for many of the plastics; however, PVC remained highly softened. Interestingly, Nylon 12 also returned its starting hardness value, even though it experienced significant mass and volume loss. This return to starting hardness values indicates that it was not a plasticizer component that was extracted. A plot showing the volume change results as a function of the mass change for the dried plastics is shown in Figure 19. The strong correlation, or linear relationship, that was observed for the elastomers and the wetted plastics, is shown to carry over into the dried state.

The glass transition temperature results for the nylons and polyamides, and the other plastic types are shown in Figures 20 and 21, respectively. As shown in Figure 20, the added ethanol produced a small reduction in T_g from the original value for three of the nylons and all of the polyamides. The notable exception is Nylon 12, in which the added ethanol raised the T_g from 260K to 300K. This increase is significant, especially since this temperature range is encountered in most ambient settings. The addition of isobutanol had no discernable effect over baseline, except for Nylon 11, where T_g was lowered by from 320K to 250K. This effect is attributed to the retention of the test fuel after drying as shown in Figure 15. For the other plastic materials (Figure 21), only ETFE, PBT and PVC showed a significant change in T_g following exposure to the test fuels. For ETFE and PBT, T_g was lowered ~16, and 40 degrees Kelvin following exposure to either test fuel. (Note that data for PBT exposed to CE10a was missing and was subsequently replaced with the CE25a result. Previous studies have shown that the properties for of PBT exposed to 10 and 25% ethanol were roughly similar.) In contrast to the other plastics, PVC showed a pronounced increase following exposure to either test fuel. This result further confirms that the PVC grade evaluated in this study was structurally degraded by the test fuels.

Compositional Changes of Exposed Neoprene, Nylon 12, NBR (GD Grade) and PVC Specimens

Several of the materials lost significant mass and volume after being dried. Four were selected for further study. They included two elastomers (neoprene and NBR (GD grade) and two plastics (Nylon 12 and PVC). Dried specimens for each material were evaluated against untreated specimens in order to elucidate compositional changes that occurred following exposure to the test fuels. Sections from the selected specimens were removed and subsequently analyzed by thermal desorption/pyrolysis gas chromatography mass spectrometry (TDP-GC-MS) using a multi-shot

pyrolysis injector (Frontier Laboratories, Ltd model EGA/PY-3030D) coupled to a GC-MS (Agilent 5975).

The specimen sections were desorbed under helium using a temperature ramp from 40 – 325 °C. The desorbed compounds were separated on a DB-5 column and analyzed with positive ion MS. The second pyrolysis step was a flash heating to 550 °C, followed by GC-MS analysis. The desorption profiles for these materials are shown in Figures 22-25. It is interesting to note the presence of the two base fuel components (isooctane and toluene) in several of the exposed specimens. For NBR (Figure 22), the measured levels of the listed additives and fuel components were appreciable but low (less than 10,000 area counts/mg). The results show that test fuels extracted the phenolic compounds used as antioxidants and undefined monomer compounds. This extraction accounts for the observed shrinkage following dry out. Low levels of phthalates, which are as added to improve plasticity, were detected in the specimens exposed to the test fuels, but not for the unexposed specimen. This lack of plasticizer detection in the untreated specimen is not considered accurate, especially since it was the only source of origin in the exposed specimens. The reason for this anomaly is attributed to the low levels of the plasticizer additive in the NBR. These levels were likely on the margin of the detection and accuracy limits of the GC-MS analyzer, and therefore of questionable value. More pronounced was the presence of isooctane in the dried specimens (and the absence of toluene). The selectivity of the NBR material for isooctane retention is not completely understood, but it does suggest that one or more of the NBR components had matching low polarity and hydrogen bonding forces that enabled attraction of isooctane, which also has low polarity and hydrogen bonding.

The results for neoprene (Figure 23) show much higher detection levels for the additive components. Here the loss of alkyl alcohols (processing aid additive) and phthalates (plasticizer

additive) with test fuel exposure is readily apparent. The dissolution and extraction of these additives account for the observed shrinkage and hardness increase in the dried specimens. Fuel retention was not observed for this material. The Nylon 12 results (Figure 24) also show high detection levels, especially for the retained fuel components. The test fuels dissolved and extracted the fatty acid amides, which are used a processing aids to reduce friction during fabrication. It is this reduction that accounts for the observed shrinkage. The phthalate plasticizers were still present in the exposed specimens, albeit at a much-reduced level for those specimens exposed to the CE10a test fuel. Nylon 12 also retained significant amounts of the base fuel components after drying. The pyrolysis GC-MS analytical method was not able to detect key additive components of PVC material as seen in Figure 25. However, significant levels of toluene were retained in the dried specimens. The reason for this selectivity is not clear. In order to better determine which PVC components were extracted by the test fuels and responsible for the observed shrinkage, it was necessary to perform a GC-MS analysis on the test fuels to determine the leached PVC components. This was accomplished by exposing one PVC specimen in each test fuel (500ml) for 4 weeks at 21°C. This data is shown in Figure 26. Here it can be clearly seen that plasticizer additives (benzyl alcohol, dodecanol, phenols, and carbonate ester) were extracted by the test fuels along with etocrylene (added for protection against ultraviolet radiation). The loss of these components accounts for the observed shrinkage and the loss of the plasticizers is responsible for the hardness increase and the increase in the glass transition temperature for the exposed PVC specimens.

CONCLUSION

This study investigated the compatibility performance of ten elastomers and eighteen plastic materials common to vehicle fueling systems. These materials were exposed to test fuels representing E10 and iBu16. The elastomer materials showed similar compatibilities with either test fuel type. These materials included two fluorocarbons, one fluorosilicone, four NBRs, neoprene, and ECO. Of these, the fluorocarbons, fluorosilicone, and an NBR/PVC blend exhibited the lowest levels of swelling (~20%). The two NBR hose materials and ECO underwent moderate (35-40%) expansion, while neoprene and HNBR swelled around 80% (which is excessive). Silicone swelled to 140% and would not be considered acceptable for many sealing and hose applications. Significant shrinkage and embrittlement were noted for the two NBR hose materials, HNBR, and neoprene indicating that plasticizer additives had been extracted by the test fuels. This behavior, however, is not necessarily indicative of poor compatibility performance, since plasticizers are often added as processing aids with the expectation that the absorbed fuel maintains volume swell and pliability of the polymer. The glass transition temperatures of the two NBR hose materials and HNBR were moderately raised following exposure to the test fuels. This change in T_g along with the observed swell may preclude these elastomers from some fuel system applications.

In contrast to the elastomers, none of the eighteen plastic materials experienced excessive swelling with the test fuels. The highest volume expansion occurred for Nylon 11 and ranged between 14-15%, while the other plastics swelled less than 10%. One plastic, the PVC material, lost significant mass and volume with exposure to the test fuels and would not be recommended for use with either

fuel type. Several of the plastics showed sensitivity to alcohol type. Nylon 6, Nylon 6/6, PARA, PPA (Dupont Zytel), and PBT underwent appreciably higher swelling in the test fuel containing ethanol than for the one containing isobutanol. For Nylon 6, Nylon 6/6, PARA, and PPA (Dupont Zytel), the higher swell, which accompanied exposure to CE10a, carried over into the dried state. Interestingly, Nylon 11 retained a higher level of CiBu16a in the dried state than CE10a which also lowered the Tg for this material. For many of the plastics, the added ethanol slightly lowered the glass transition temperature, which was much less impacted by isobutanol. PVC was the exception as the both hardness and Tg were increased after exposure due to extraction of plasticizer additives.

ACKNOWLEDGEMENTS

This effort was partially sponsored by Butamax Advanced Biofuels, LLC. A portion of this material was also based upon work supported by the U.S. Department of Energy's Office of Energy Efficiency and Renewable Energy (EERE) Bioenergy Technologies Office. The authors are grateful for encouragement and support by Tim Theiss and Brian West (Oak Ridge National Laboratory) and from guidance by Steve Abbott (Hansen Solubility Team). Oak Ridge National Laboratory is a multi-program laboratory operated by UT-Battelle for the U. S. Department of Energy under contract DE-AC0500OR22725.

REFERENCES

(1) Energy Independence and Security Act of 2007: A Summary of Major Provisions, CRS Report for Congress, Order Code RL34294, Dec. 21, 2007.

(2) Federal Register **1979**, 44 (680, 20777-20778, Notice April 6, 1979; Federal Register **1982**, 47 (65), 14596-14597; Regulation of Fuel and Fuel Additives: Modification to Octamix Waiver (TXCeed), Federal Register **2012**, 77 (110), 33733-33735.
(3) Touchet, P., Zanadis, B., Fischer, M., and Gatza, P. E., Materials Compatibilities Studies with Fuel/Alcohol Mixtures, Technical Report 2366, U. S. Army Mobility Equipment Research and Development Command, Fort Belvoir, VA, July 1982.
(4) Karg, R. F., Hill, C., Dosch, K., and Johnson, B., "Ultra-high CAN Polymer in Fuel System Application," SAE Technical Paper 900196, 1990, doi:10.4271/900196.
(5) Abu-Isa, I., "Effects of Mixtures of Gasoline With Methanol and With Ethanol on Automotive Elastomers," SAE Technical Paper 800786, 1980, doi:10.4271/800786.
(6) Micallef, G. and Weimann, A., "Elastomer Selection for Bio-fuel Requires a System Approach," Sealing Technology, January 2009.
(7) Ertekin, A. and Sridhar, N., "Performance of Elastomeric Materials in Gasoline-Ethanol Blends-A Review," Paper no. 09533, CORROSION 2009 Annual Conference and Exhibition, NACE International, Atlanta, 2009.
(8) Stephens, R. D., "Fuel and Permeation Resistance of Fluoroelastomers to Ethanol Blends," ACS Technical Meeting of the Rubber Division, Cincinnati, OH, October 2006.
(9) Nersasian, A., "The Use of Toluene/Isooctane/Alcohol Blends to Simulate the Swelling Behavior of Rubbers in Gasoline/Alcohol Fuels," SAE Technical Paper 800790, 1980, doi:10.4271/800790.
(10) Nihalani, I., Paulmer, R., and Rao, Y., "Compatibility of Elastomeric Materials with Gasohol," SAE Technical Paper 2004-28-0062, 2004, doi:10.4271/2004-28-0062.
(11) Jones, B., Mead, G., Steevens, P., and Connors, C., "The Effects of E20 on Elastomers Used in Automotive Fuel System Components," Minnesota Center for Automotive Research, Minnesota Center for Automotive Research, Minnesota State University, Mankato, February 22, 2008.
(12) Kass, M. et al., Compatibility of Elastomers with Test Fuels of Gasoline Blended with Ethanol, Sealing Technology, 7-12, December 2012.
(13) Durbin, T. D., Georgios, K., Norbeck, J. M., Park, C. S., Castillo, J., Rheem, Y., Bumiller, K., Yang, J., Van, V., Hunter, K. Material Compatibility Evaluation for Elastomers, Plastics and Metals Exposed to Ethanol and Butanol Blends. *Fuel* 163 (2016) 248–259
(14) Koch, W. H, Baustian, J. J. Isobutanol: Biofuel of the Future. PEI Journal **2012**, 4, 28-34.
(15) Kass, M. D., Janke, C., Theiss, T., Baustian, J., Wolf, L., Koch, W. Compatibility Assessment of Plastic Infrastructure Materials with Test Fuels Representing E10 and iBu16. *SAE Int. J. Fuels Lubr*. 8(1):2015, doi:10.4271/2015-01-0894
(16) Kass, M. D., Janke, C., Theiss, T., Baustian, J., Wolf, L., Koch, W. Compatibility Assessment of Plastic Infrastructure Materials Test Fuels Representing Gasoline Blends Containing Ethanol and Isobutanol. *SAE Int. J. Fuels Lubr*. 7(2):2014, doi:10.4271/2014-01-1462
(17) SAE Surface Vehicle Recommended Practice, "Gasoline, Alcohol, and Diesel Fuel Surrogates for Materials Testing," SAE Standard J1681, Rev. Jan. 2000.

(18) Kass, M. D., Theiss, T. J., Janke C. J., Pawel S. J., and Lewis S. A., Intermediate Ethanol Blends Infrastructure Materials Compatibility Study: Elastomers, Metals, and Sealants, ORNL/TM-2010/88 March 2011.
(19) Underwriters Laboratories. *Standard for Power-operated Dispensing Devices for Gasoline/Ethanol Blends with Nominal Ethanol Concentrations up to 85% (E0 - E85)* UL 87A. 2015.
(20) ASTM D471-16a, Standard Test Method for Rubber Property—Effect of Liquids, ASTM International, West Conshohocken, PA, 2016, www.astm.org
(21) ASTM D2240, Standard Test Method for Rubber Property-Durometer Hardness, ASTM International, West Conshohocken, PA, 2016, www.astm.org

Table 1. Formulations used to make 1 liter of aggressive ethanol or aggressive isobutanol (Units are in grams.)

Component	Aggressive Ethanol	Aggressive Isobutanol
CDA Ethanol Reagent grade isobutanol	781.6 --------	------- 797.7
De-ionized water	8.103	7.987
Sodium chloride	0.004	0.004
Sulfuric acid	0.021	0.021
Glacial acetic acid Isobutyric acid	0.061 -------	------- 0.088

Table 2. Listing of each elastomer type and its corresponding application

Elastomer Type	Manufacturer and/or Trade Name	Application
Fluorocarbon	Viton A401C	Seals and o-rings
Fluorocarbon	Viton B601	Seals and o-rings
Fluorosilicone	Parker LM155	Seals and o-rings
Neoprene	McMaster-Carr 5122K21	Legacy fuel lines and seals
NBR SE Grade	Parker	Small engine hose material
NBR GD Grade	Parker	Gasoline dispenser hose material
Silicone	Parker S0604	Seal material for non-road engines
Hydrogenated NBR	Parker	Fuel lines, seals, and o-rings
Blend of NBR/PVC, (OZO)	Parker	Seals and tank liners
Epichlorohydrin/ethylene oxide (ECO)	Parker	Legacy gasket material

Table 3. Infrastructure Plastic Materials and Their Applications

Plastic Type	Trade Name	Application(s)
Nylons and Polyamides		
Nylon 6		Plastic piping and seal material
Nylon 6/6		Plastic piping and seal material
Nylon 11		Fuel tank material
Nylon 12		Fuel lines and plastic piping material
Polyarylamide (PARA)	Solvay IXEF	Fuel pump housings
Polyphthalamide (PPA)	Dupont Zytel	Engine covers and housings
Polyphthalamide (PPA)	Solvay Amodel	Fittings, fuel and vapor lines, carburetors, and throttle bodies
Other Key Plastics		
Polyphenylene sulfide (PPS)	Techtron™	Liners
Polytetrafluoroethylene (PTFE)	Teflon™	Liners and seal material
Polyvinylidene fluoride (PVDF)	Kynar™	Liners and pipe material
Ethylene tetrafluoroethylene (ETFE)	Tefzel	Valve lining and pump components
Polybutylene terephthalate (PBT)	Celanex	Automotive connectors
High Density Polyethylene (HDPE)		Fuel tanks
Polyoxymethylene (POM) or acetal	Delrin II™	Fuel line valves, pump and tank components
Polyvinyl Chloride (PVC)		Underbody coatings and sealants
Polyetherimide (PEI)	Ultem 1010	Throttle bodies, ignition components, and sensor housings
Polyether ether ketone (PEEK)	Solvay KT-820NT	Oil and fuel system components, lightweight structural components
Glass fiber/phenol formaldehyde	Norplex NP504	Lightweight structural components

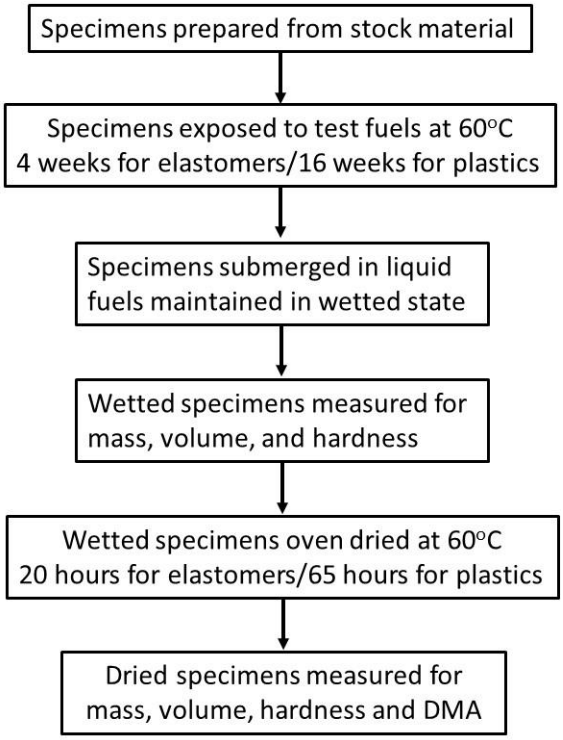

Figure 1. Flow chart showing the exposure protocol and test methods.

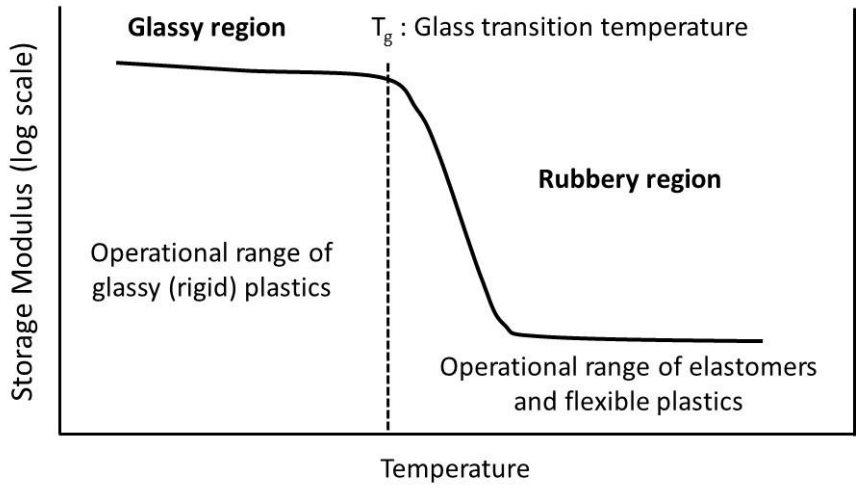

Figure 2. Generic representation of the storage (Young's) modulus as a function of temperature for most polymeric materials. At Tg, the polymer transitions from a rigid (glassy) state to a rubbery (highly flexible) one.

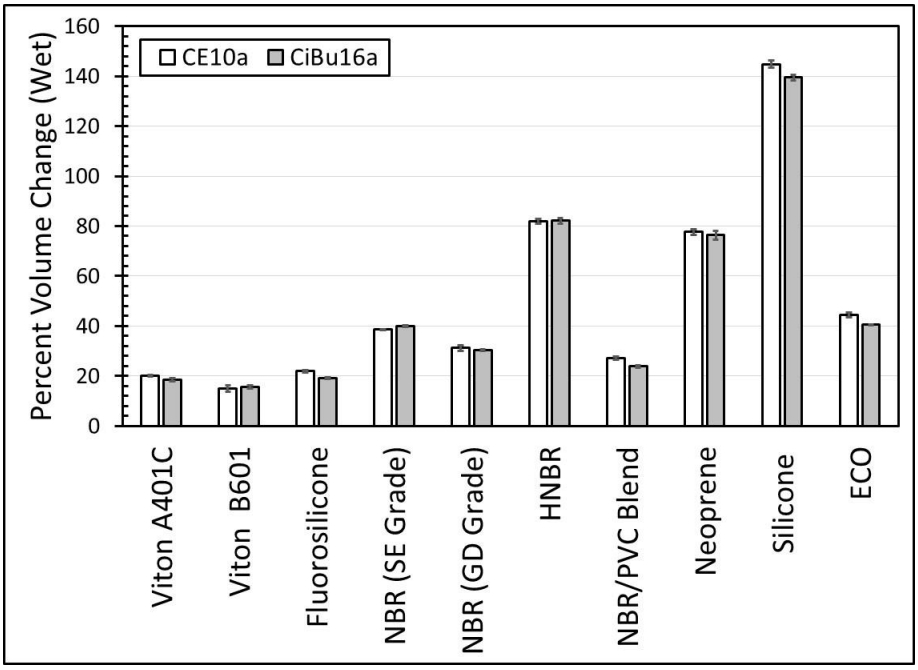

Figure 3. The percent volume change (compared to baseline values) for the elastomers in the wetted state exposed to either CE10a or CiBu16a.

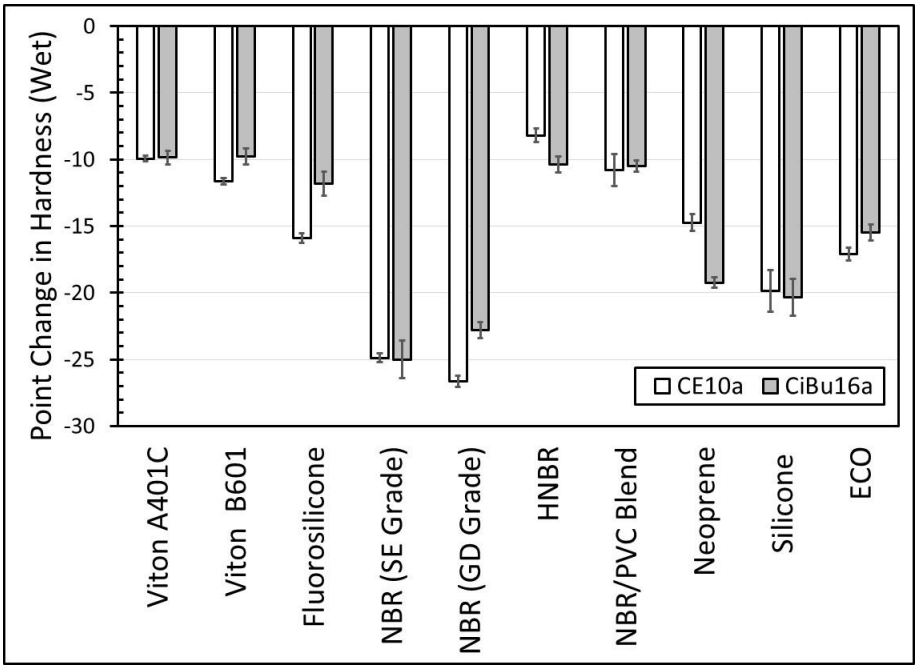

Figure 4. The point change in hardness (compared to baseline values) for the elastomers in the wetted state following exposure to CE10a and CiBu16a.

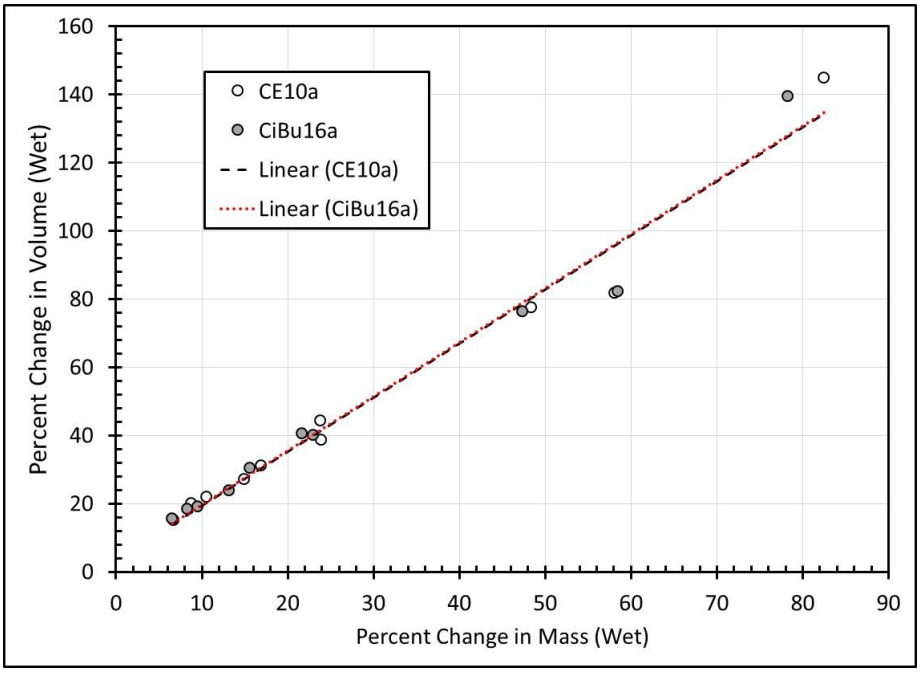

Figure 5. Relationship between the mass and volume change for the elastomers exposed to CE10a and CiBu16a in the wetted state. The curve shows a strong linear dependency of volume with mass that is independent of fuel type.

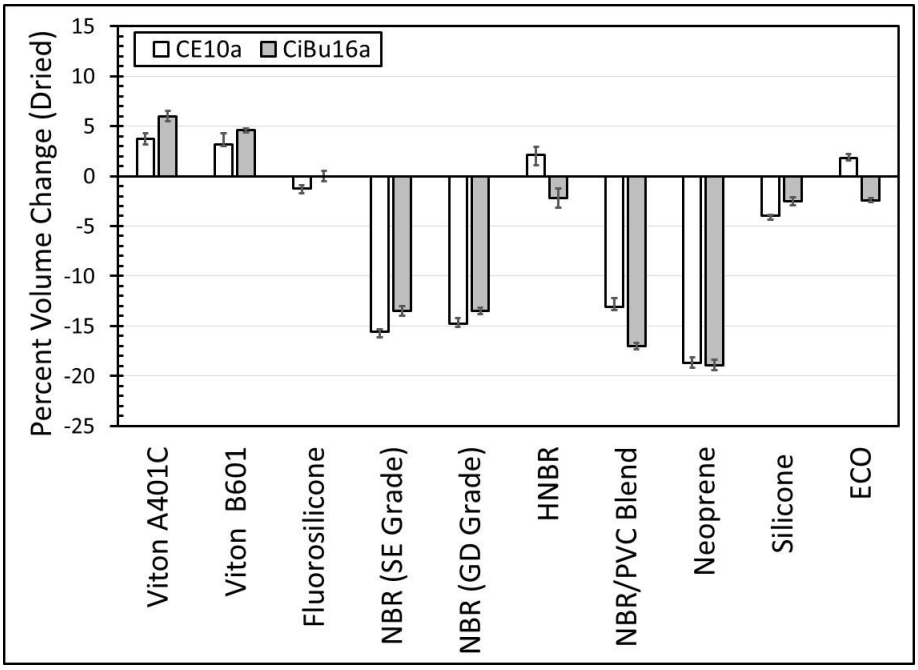

Figure 6. Percent change in volume for the elastomer specimens after drying at 60°C for 20 hours. The elastomers were exposed to CE10a or CiBu16a.

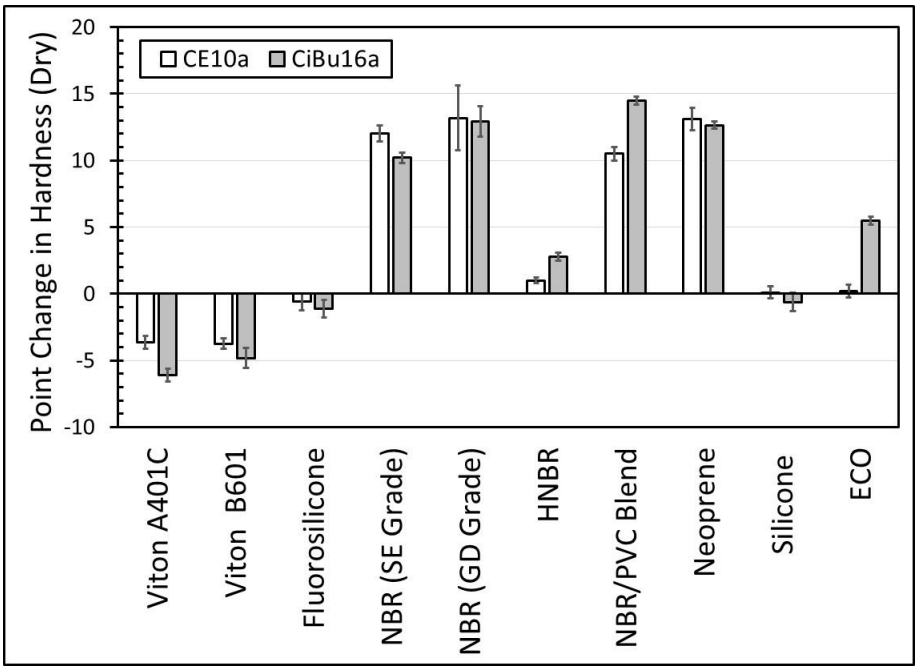

Figure 7. The point change in hardness results (compared to the original values) for the elastomer materials exposed to CE10a and CiBu16a when wetted and after being dried at 60ºC for 20 hours.

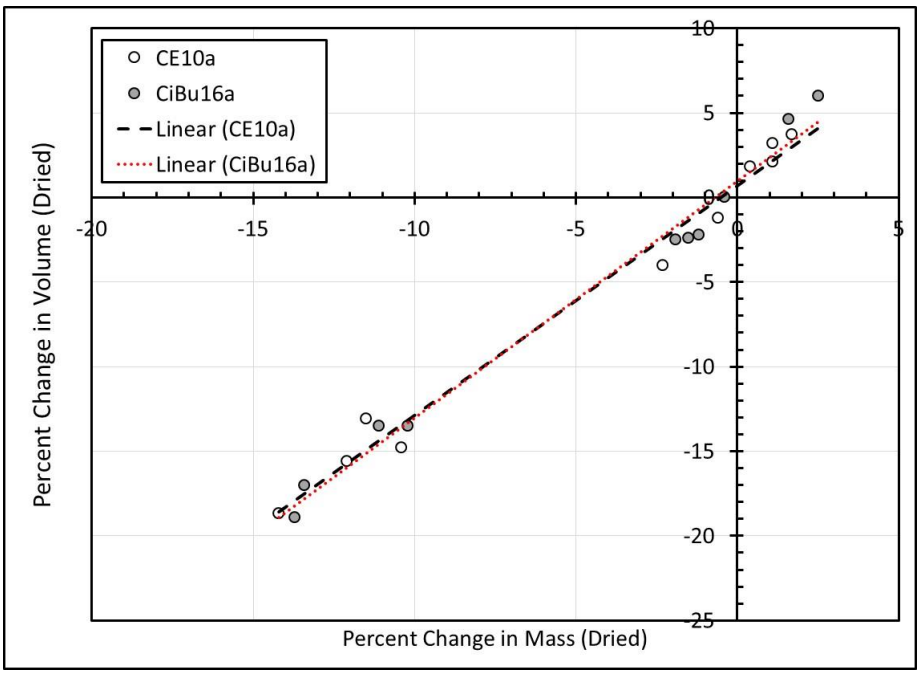

Figure 8. Relationship between the mass and volume change for the elastomers exposed to CE10a and CiBu16a in the dried state. The curve shows a strong linear dependency of volume with mass that is independent of fuel type.

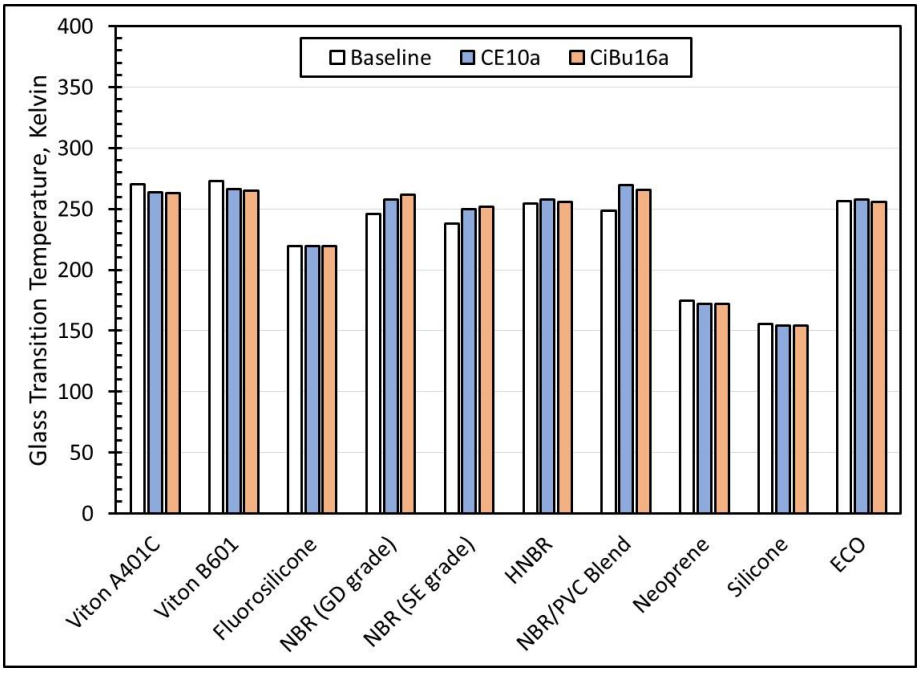

Figure 9. The glass transition temperatures for the elastomer materials. For each elastomer type, the baseline results are depicted alongside those for CE10a and CiBu16a. The wetted specimens were dried at 60ºC for 20 hours prior to measurement.

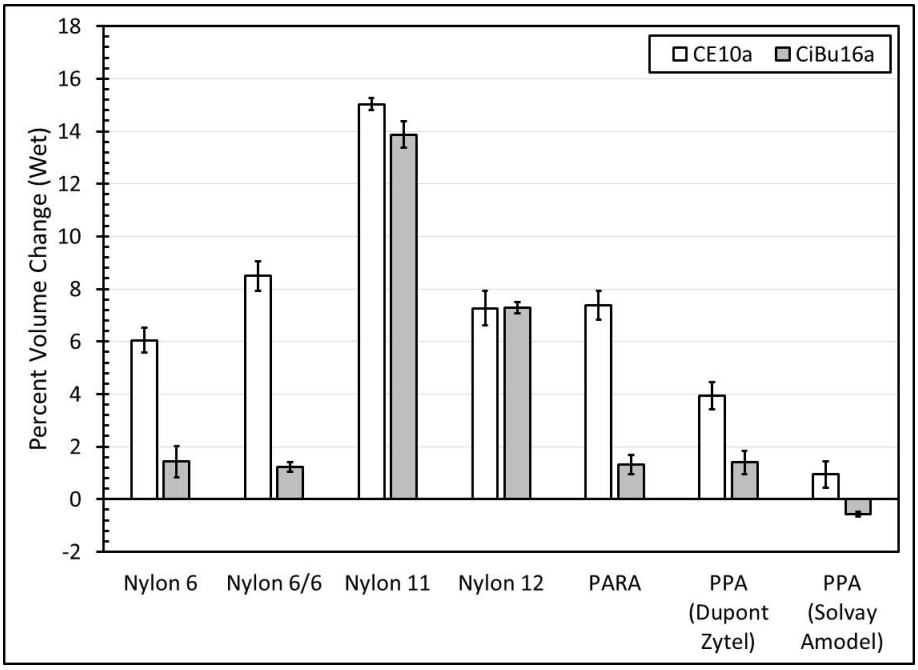

Figure 10. The percent volume change (compared to baseline values) for the nylons and other polyamides in the wetted state exposed to either CE10a or CiBu16a.

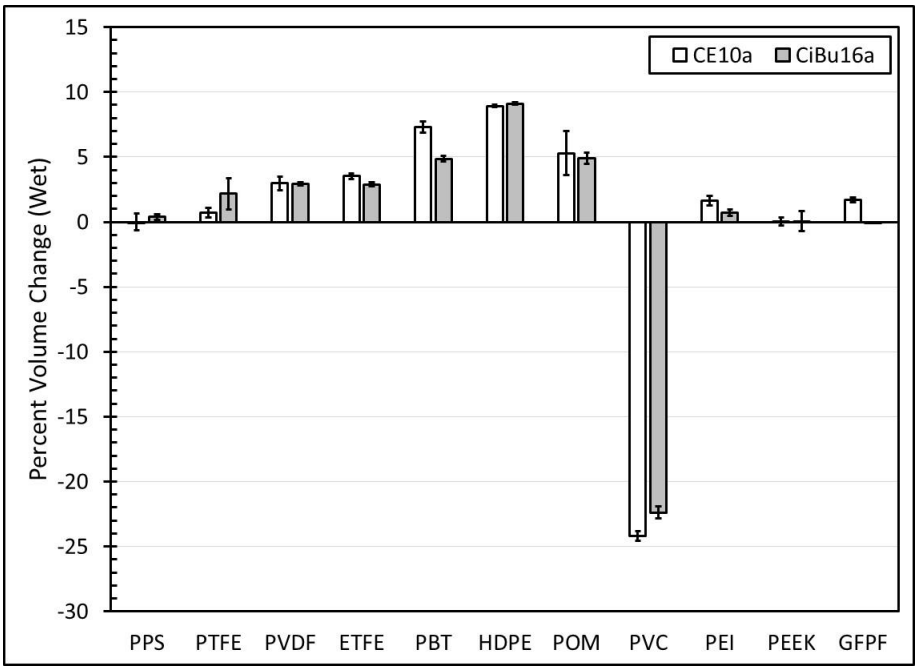

Figure 11. The percent volume change (compared to baseline values) for other key fuel system plastics in the wetted state exposed to either CE10a or CiBu16a.

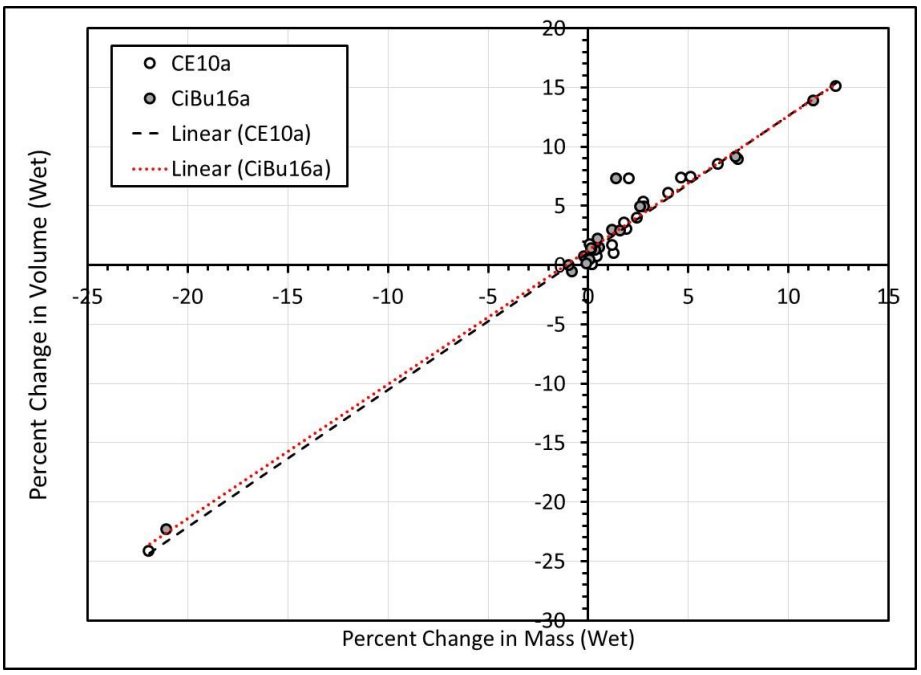

Figure 12. Relationship between the mass and volume change for the plastics exposed to CE10a and CiBu16a in the wetted state. The curve shows a strong linear dependency of volume with mass that is independent of fuel type.

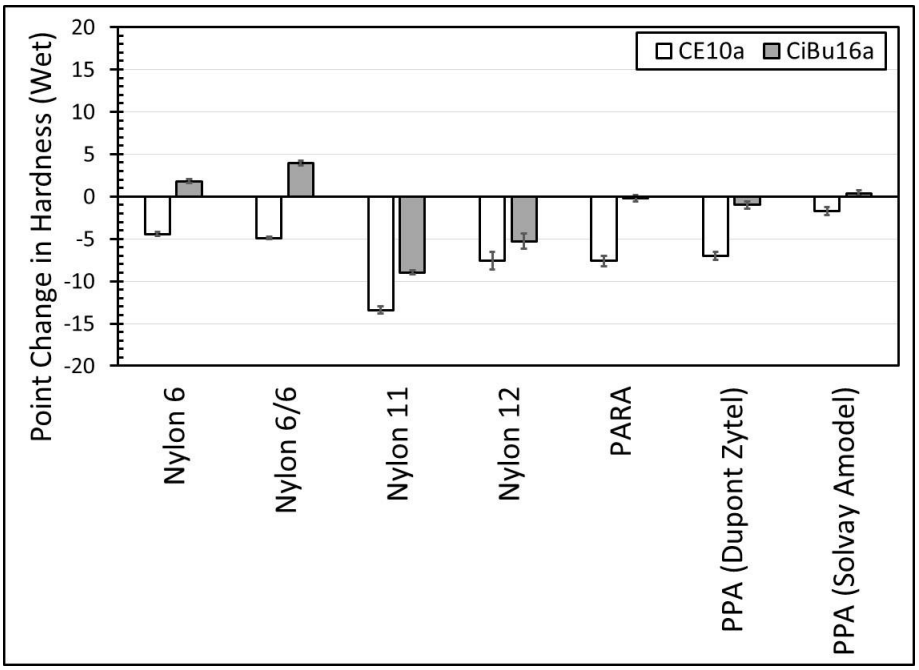

Figure 13. The point change in hardness results (compared to the original values) for the nylons and polyamides exposed to CE10a and CiBu16a and measured while in the wetted state.

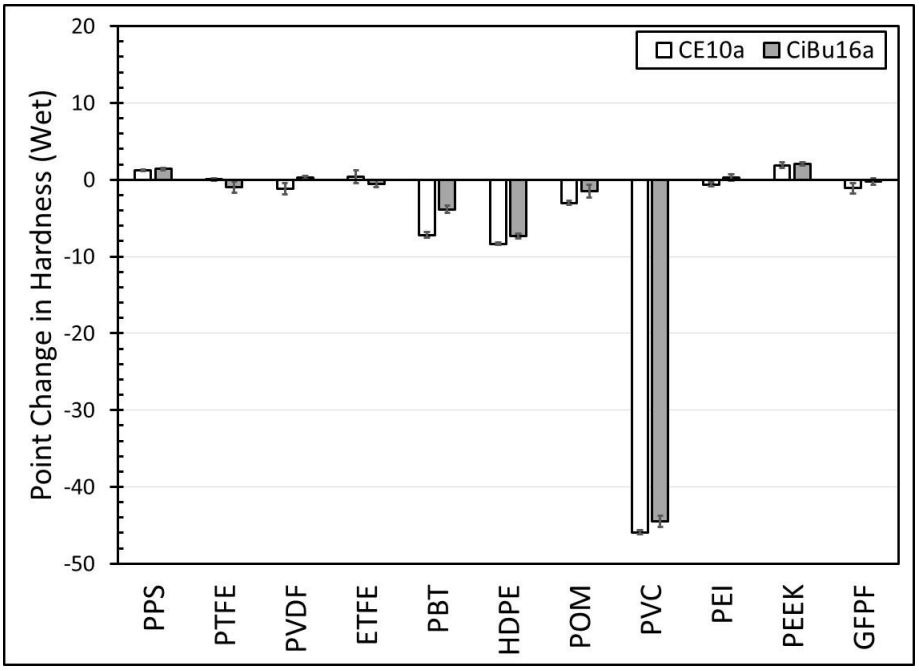

Figure 14. The point change in hardness results (compared to the original values) for other fuel system plastics exposed to CE10a and CiBu16a and measured while in the wetted state.

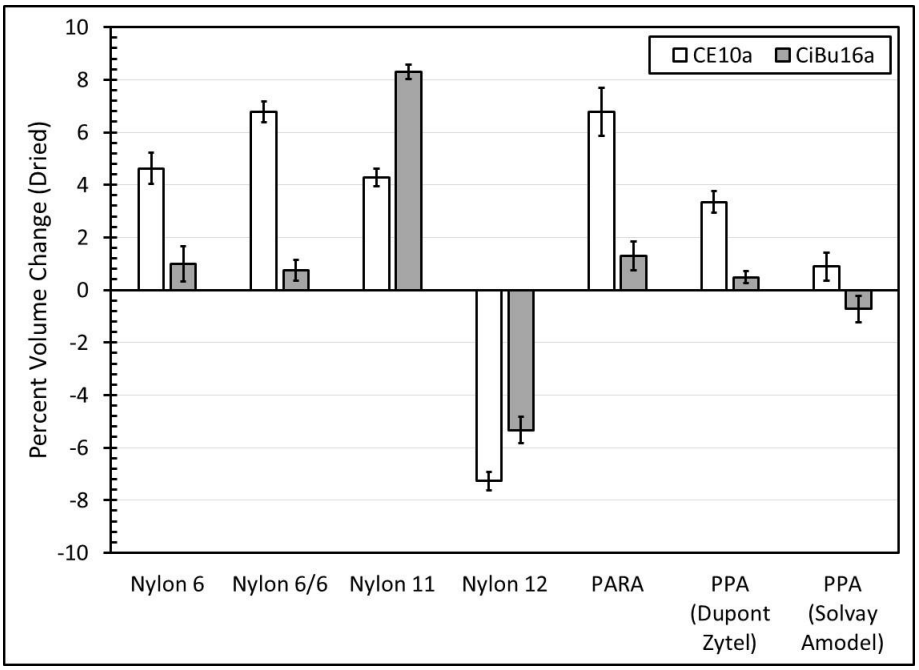

Figure 15. The percent volume change (compared to baseline values) for the nylon and polyamide plastics exposed to either CE10a or CiBu16a and then dried at 60ºC for 65 hours.

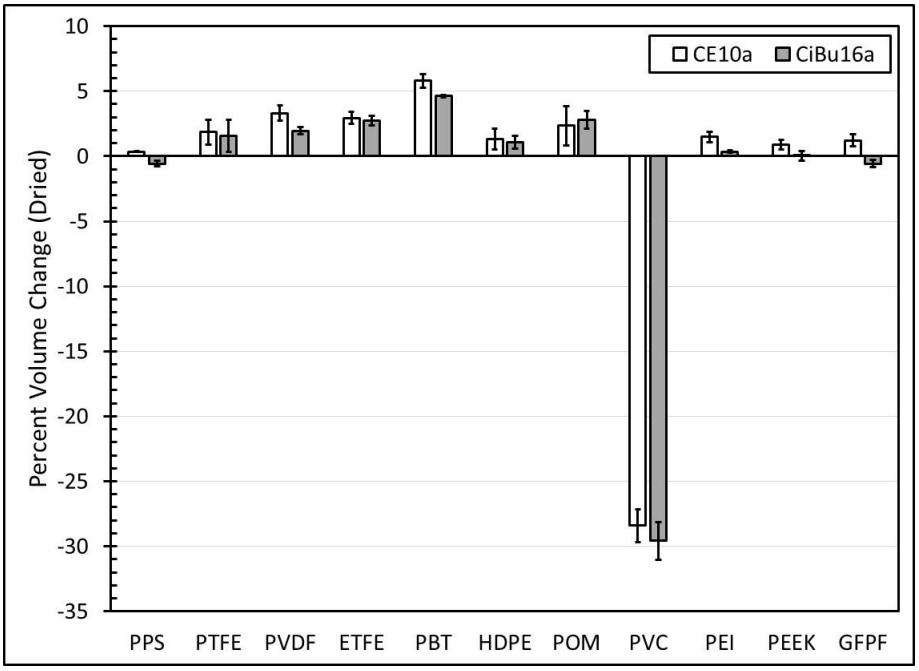

Figure 16. The percent volume change (compared to baseline values) for other key fuel system plastics exposed to either CE10a or CiBu16a and then dried at 60ºC for 65 hours.

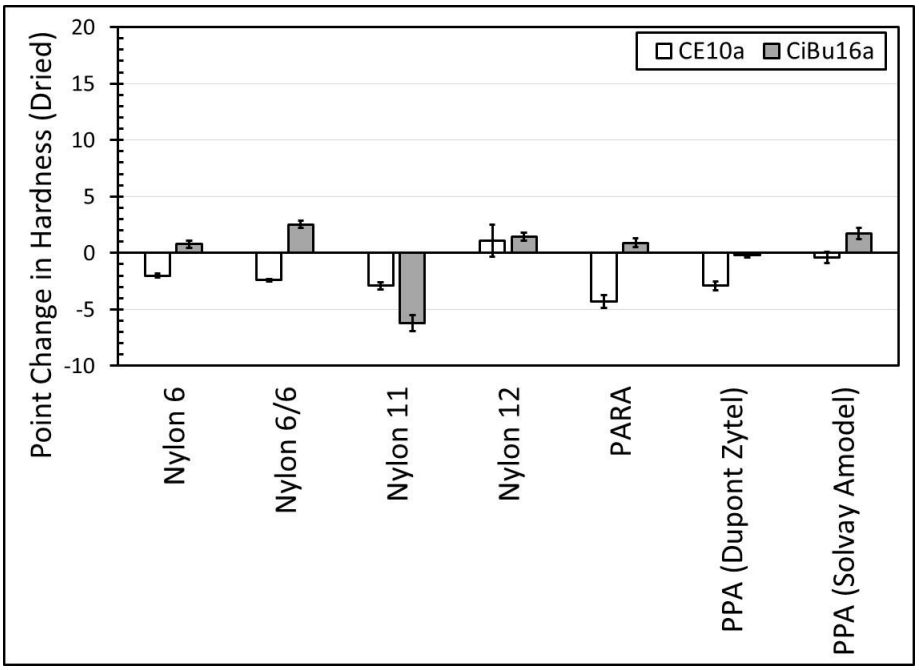

Figure 17. The point change in hardness results (compared to baseline values) for the nylon and polyamide plastics exposed to either CE10a or CiBu16a and then dried at 60ºC for 65 hours.

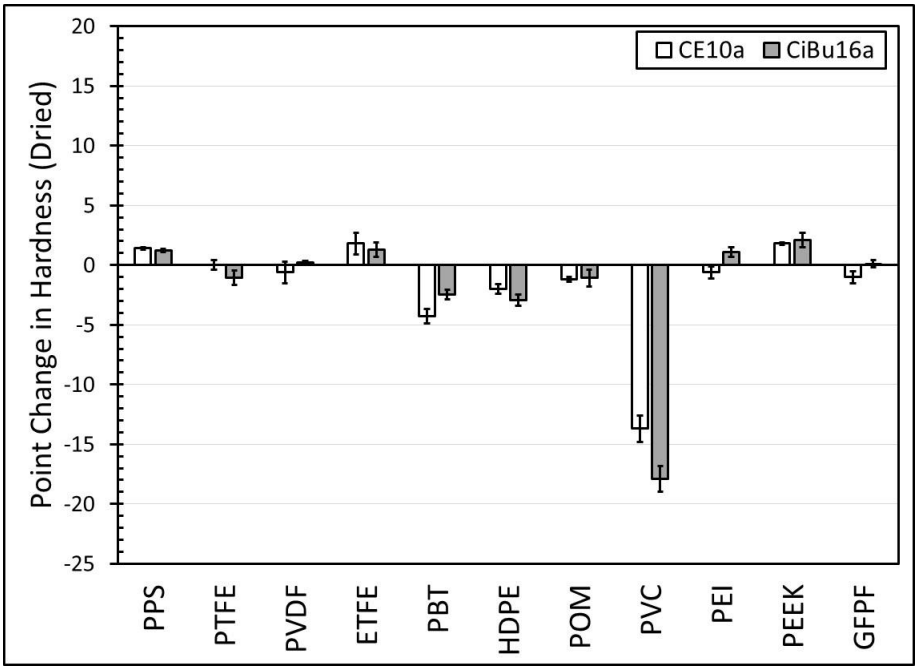

Figure 18. The point change in hardness results (compared to baseline values) for other key fuel system plastics exposed to either CE10a or CiBu16a and then dried at 60ºC for 65 hours.

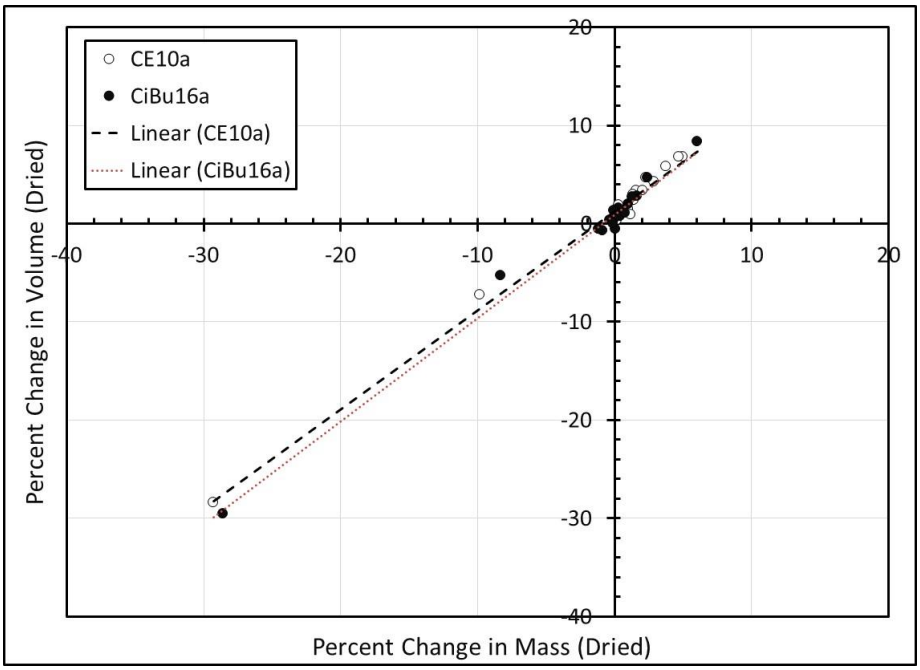

Figure 19. Relationship between the mass and volume change for the plastics exposed to CE10a and CiBu16a in the dried state. The curve shows a strong linear dependency of volume with mass that is independent of fuel type.

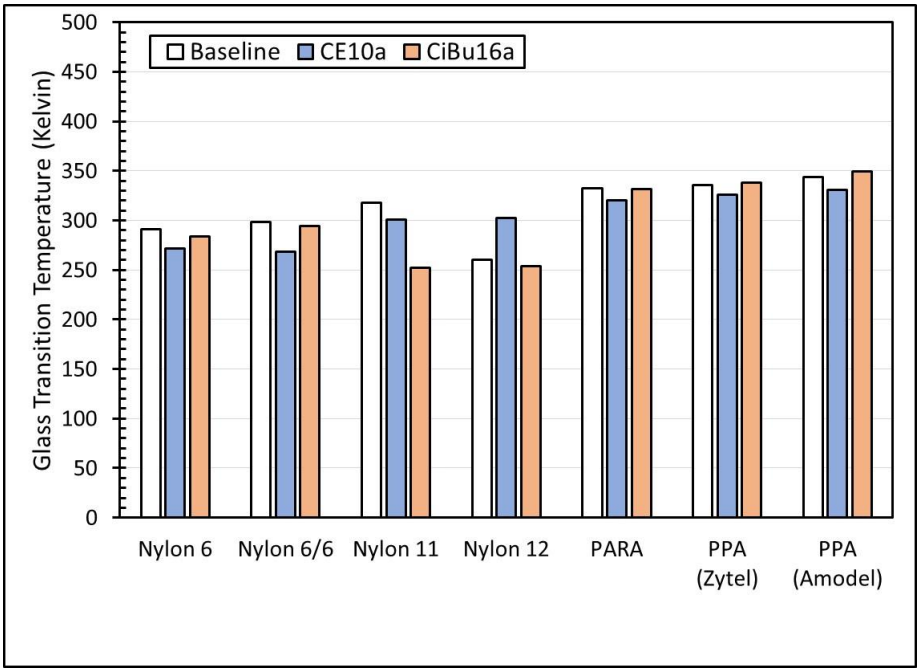

Figure 20. The glass transition temperatures for the nylons and polyamides. For each plastic type, the baseline results are depicted alongside those for CE10a and CiBu16a. The wetted specimens were dried at 60°C for 65 hours prior to measurement.

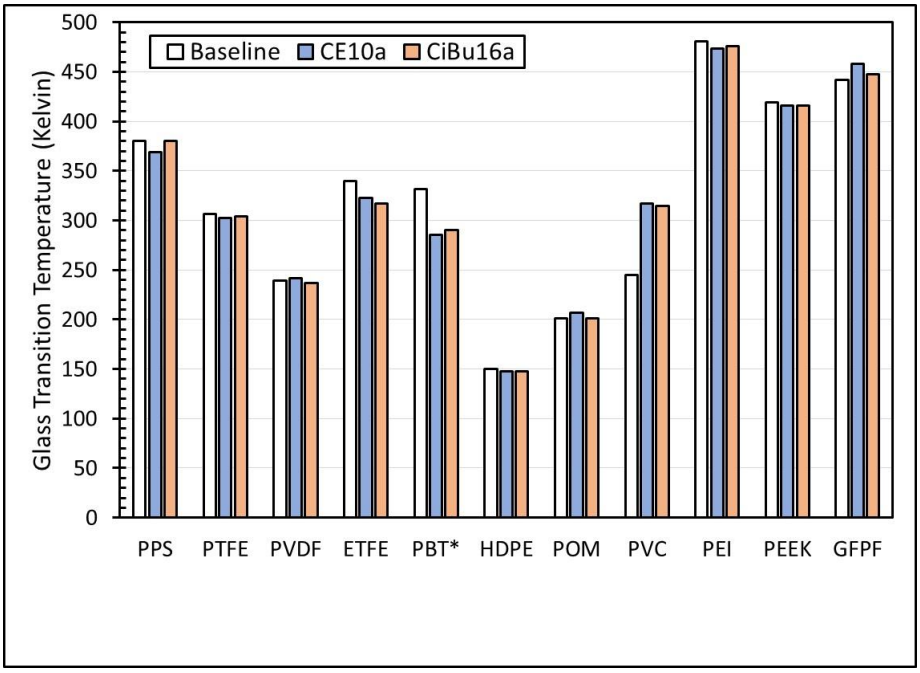

Figure 21. The glass transition temperatures for the other plastic materials. For each plastic type, the baseline results are depicted alongside those for CE10a and CiBu16a. The wetted specimens were dried at 60°C for 65 hours prior to measurement. Note that the result for the CE10a exposure to PBT was replaced with the value obtained for CE25a exposure due to specimen mishandling.

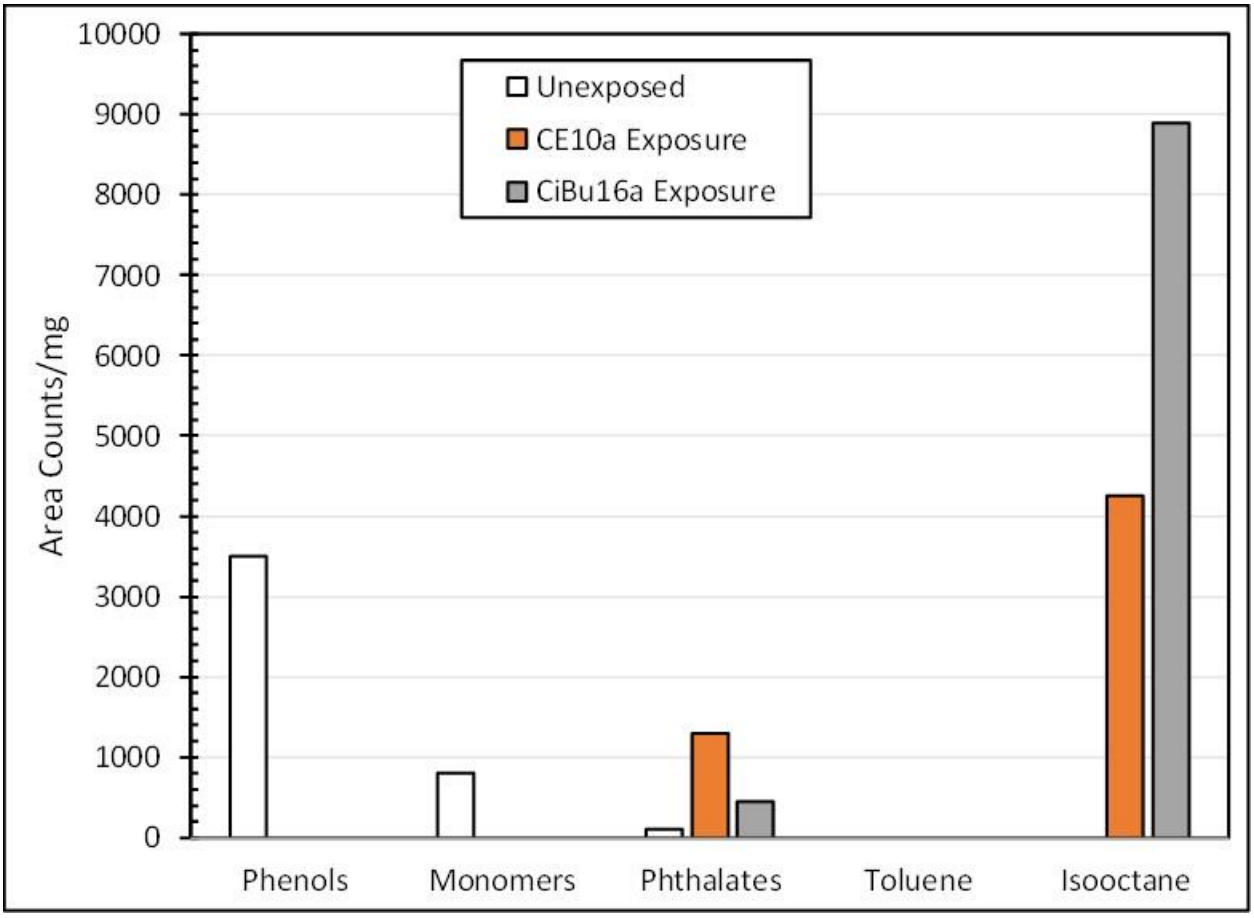

Figure 22. Results of the thermal desorption/pyrolysis gas chromatography mass spectrometry analysis on the NBR material. For each plastic type, the unexposed results are depicted alongside those for specimens exposed to CE10a and CiBu16a. The exposed specimens were dried at 60°C for 65 hours prior to measurement.

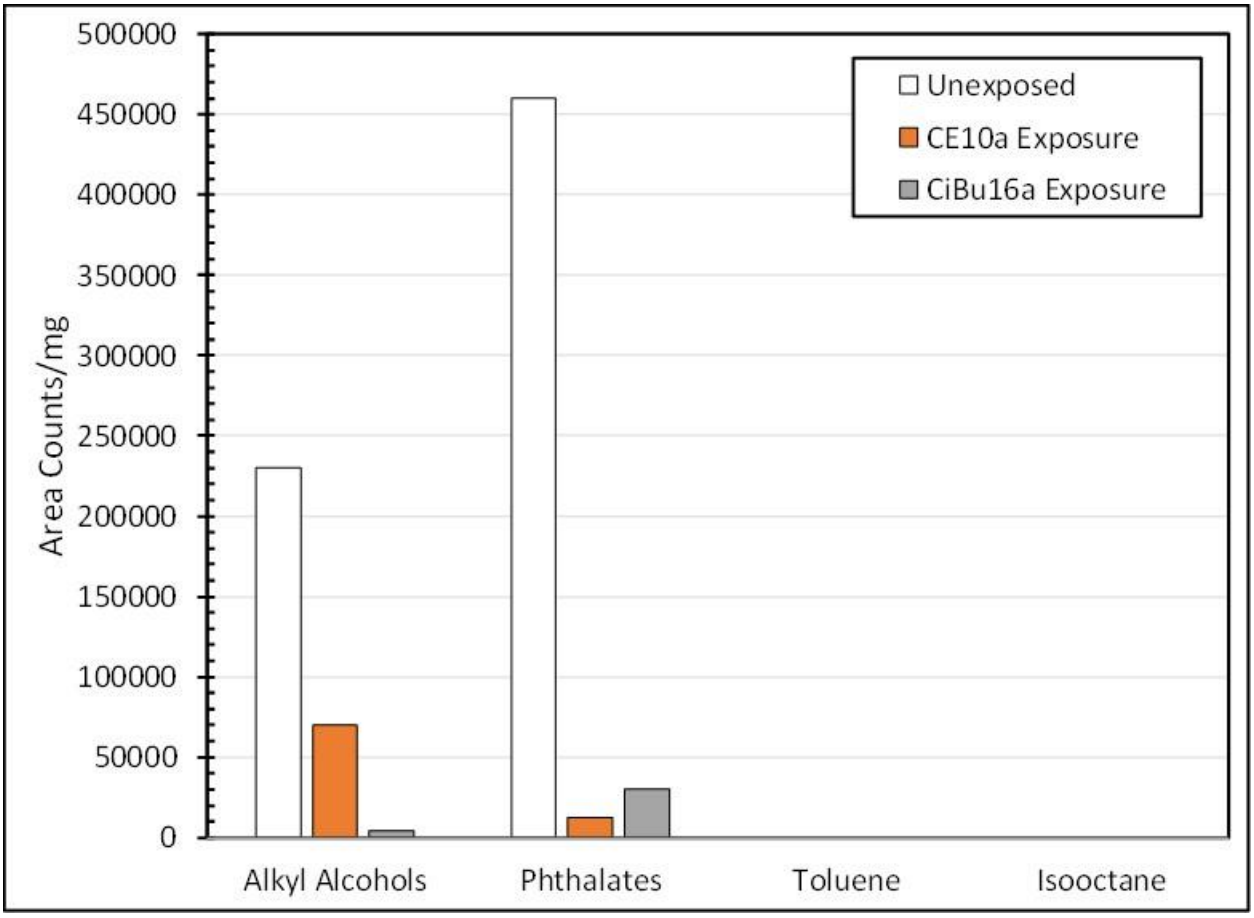

Figure 23. Results of the thermal desorption/pyrolysis gas chromatography mass spectrometry analysis on the neoprene material. For each plastic type, the unexposed results are depicted alongside those for specimens exposed to CE10a and CiBu16a. The exposed specimens were dried at 60ºC for 65 hours prior to measurement.

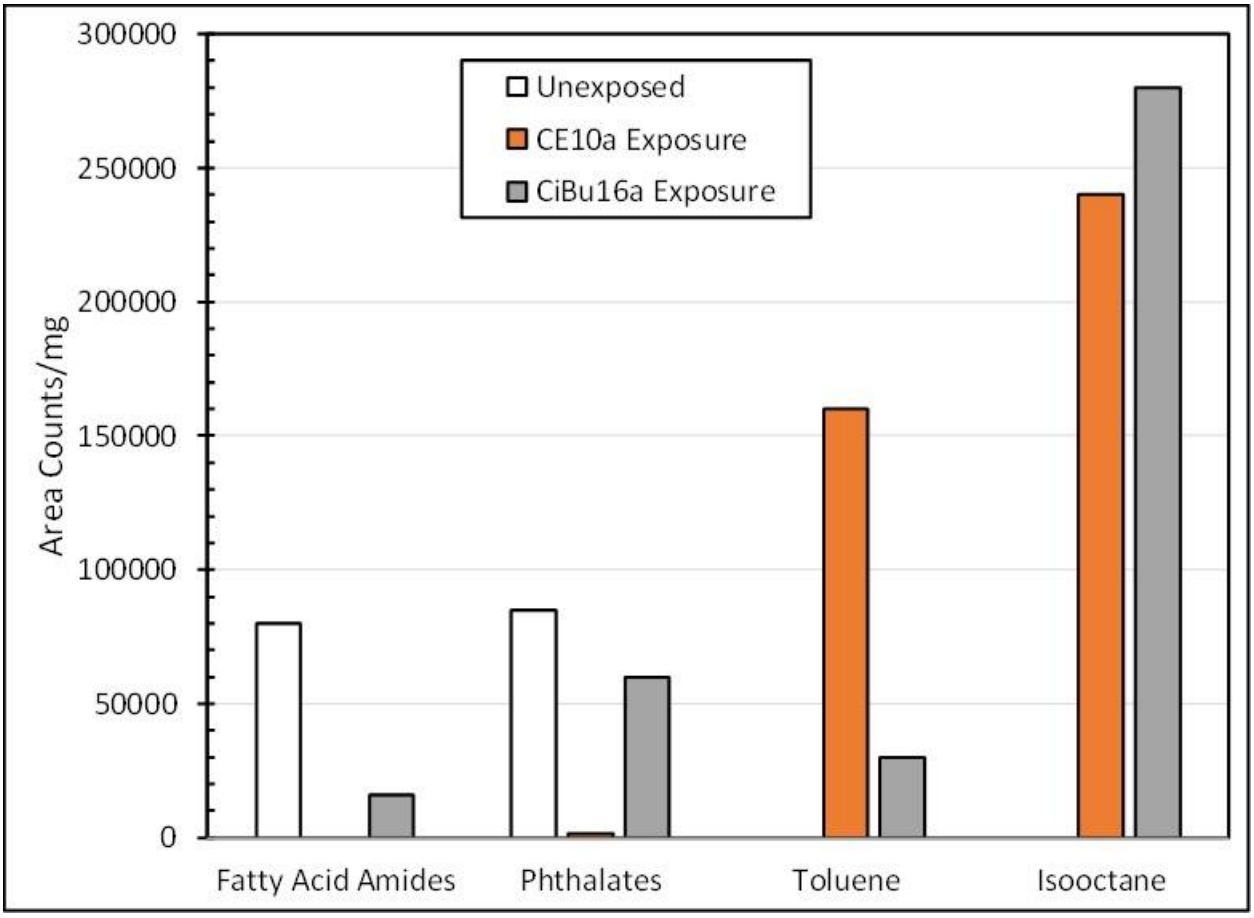

Figure 24. Results of the thermal desorption/pyrolysis gas chromatography mass spectrometry analysis on the Nylon 12 material. For each plastic type, the unexposed results are depicted alongside those for specimens exposed to CE10a and CiBu16a. The exposed specimens were dried at 60ºC for 65 hours prior to measurement.

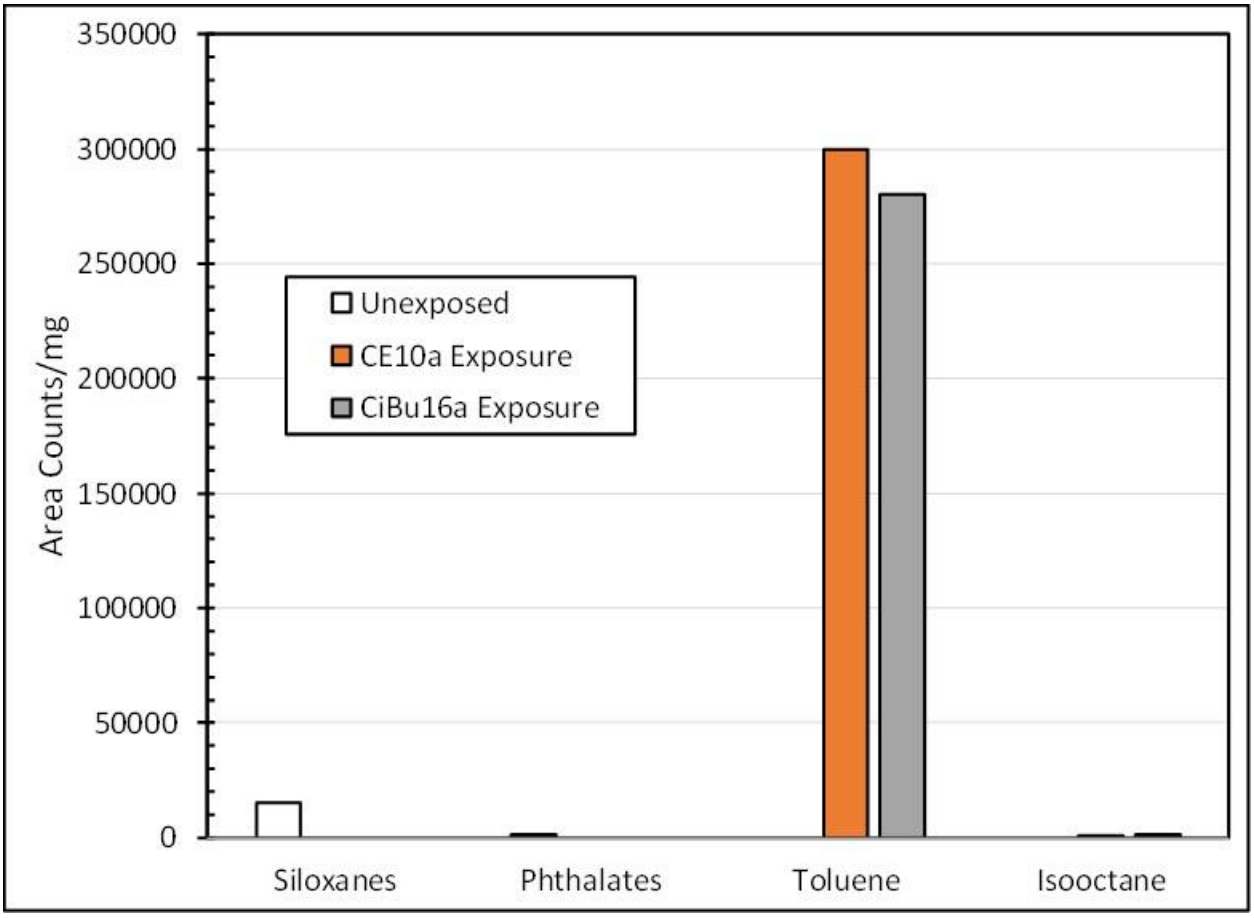

Figure 25. Results of the thermal desorption/pyrolysis gas chromatography mass spectrometry analysis on the PVC material. For each plastic type, the unexposed results are depicted alongside those for specimens exposed to CE10a and CiBu16a. The exposed specimens were dried at 60°C for 65 hours prior to measurement.

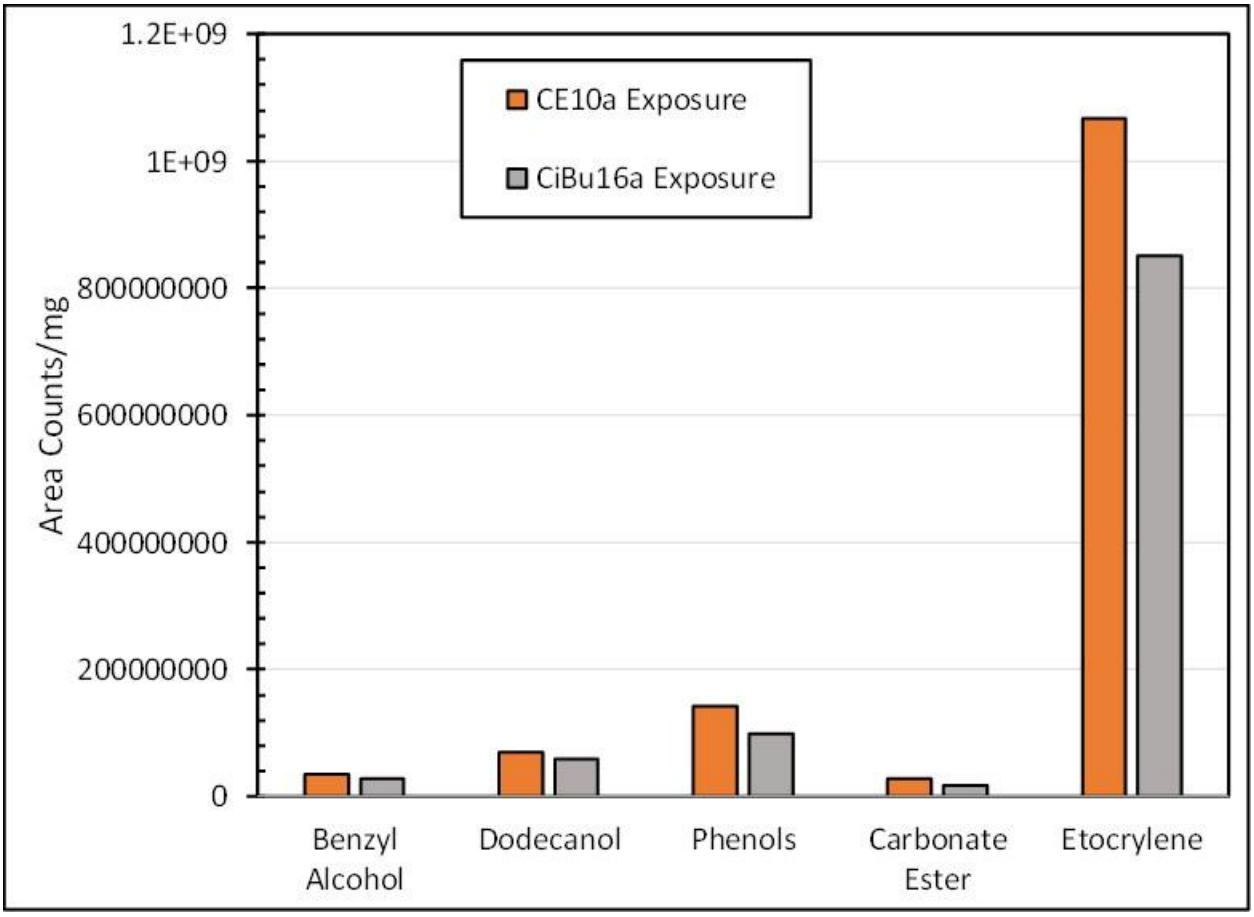

Figure 26. Results of gas chromatography mass spectrometry analysis on the test fuels exposed to the PVC material. The listed compounds were extracted from the PVC specimens and present as dissolved substances in the test fuels.